

About Low Frequency Resonances of Elastic Spheroidal Shells, Irradiating and Establishing by Harmonic and Pulse Signals

A. A. Kleshchev*, E. I. Kuznetsova

Saint – Petersburg State Navy Technical University, Russia, 190008, Saint , Petersburg Lotsmanskaya st., 3

Abstract The done before analysis of the low frequency resonances of the elastic spheroidal bodies, irradiating and establishing by the harmonic signal[1], supplemented with the research of the elastic spheroidal shell, irradiating and establishing by the pulse signal.

Keywords Diffraction, Lamé Constants, Potential, Elastic Shell, Boundary Conditions

1. Introduction

In the paper is showing, what the low frequency resonances of the elastic prolate spheroidal shells are discovered by the axisymmetrical irradiation.

2. The First Part of the Article Investigates the Results of the Numerical Experiment for the Determination of the Low Frequency Resonances of the Elastic Spheroidal Shell, Irradiating and Establishing by the Harmonic Signal

The frequencies of the first resonances of the elastic oscillations of spheroidal bodies may be established very exactly with the help of their sections of a radiation and scattering (of the integral characteristics)[2, 3]. These results may be obtained and by analysis of the angular characteristics of the radiation $F(\theta, \varphi)$ and the scattering $\psi(\theta, \varphi)$ of the sound for these bodies. Let us consider a scatterer in the form of an isotropic spheroidal shell, illuminating along axis of the rotation of the shell (the axis – symmetrical problem). All the potentials, including the plane

wave potential Φ_0 , the scattered wave potential Φ_1 , the scalar shell potential Φ_2 , the component A_φ of the vector \vec{A} potential and the potential Φ_3 of the gas filling the shell, can be expanded in spheroidal wave functions[2, 3]:

$$\Phi_0 = 2 \sum_{n=0}^{\infty} i^{-n} \bar{S}_{0,n}(C, 1) \bar{S}_{0,n}(C, \eta) R_{0,n}^{(1)}(C, \xi); \quad (1)$$

$$\Phi_1 = 2 \sum_{n=0}^{\infty} B_n \bar{S}_{0,n}(C, \eta) R_{0,n}^{(3)}(C, \xi); \quad (2)$$

$$\Phi_2 = 2 \sum_{n=0}^{\infty} [C_n R_{0,n}^{(1)}(C_l, \xi) + D_n R_{0,n}^{(2)}(C_l, \xi)] \bar{S}_{0,n}(C_l, \eta); \quad (3)$$

$$A_\varphi = 4 \sum_{n=1}^{\infty} [F_n R_{1,n}^{(1)}(C_l, \xi) + G_n R_{1,n}^{(2)}(C_l, \xi)] \bar{S}_{1,n}(C_l, \eta); \quad (4)$$

$$\Phi_3 = 2 \sum_{n=0}^{\infty} E_n R_{0,n}^{(1)}(C_l, \xi) \bar{S}_{0,n}(C_l, \eta), \quad (5)$$

where $C_l = k_l h_0$, k_l – the wavenumber of the longitudinal elastic wave, h_0 – semi – focus distance; $C_t = k_t h_0$, k_t – the wavenumber of the transverse elastic wave; $C = k h_0$, k – the wavenumber of the sound wave in the fluid; $C_1 = k_1 h_0$, k_1 – the wavenumber of the sound wave in the gas filling the shell; $B_n, C_n, D_n, F_n, G_n, E_n$ are unknown expansion coefficients. The expansion coefficients are determined from the physical boundary conditions preset at the two surfaces of the shell (ξ_0 and ξ_1):

* Corresponding author:
 alexalex-2@yandex.ru (A. A. Kleshchev)
 Published online at <http://journal.sapub.org/ijtmp>
 Copyright © 2013 Scientific & Academic Publishing. All Rights Reserved

1. the continuity of the normal displacement component at both of the boundaries, ξ_0 and ξ_1 ;
2. the identity between the normal stress in the elastic shell and the sound pressure in the liquid (ξ_0) or in the gas (ξ_1);
3. the absence of tangential stress at both of the shell boundaries, ξ_0 and ξ_1 .

The corresponding expressions for the boundary conditions have in the form[2]:

$$-(h_\xi)^{-1}(\partial/\partial\xi)(\Phi_0 + \Phi_1) = -(h_\xi)^{-1}(\partial\Phi_2/\partial\xi) + (h_\eta h_\varphi)^{-1}[(\partial/\partial\eta)(h_\varphi A_\varphi)] \text{ by } \xi = \xi_0; \quad (6)$$

$$-(h_\xi)^{-1}(\partial\Phi_3/\partial\xi) = -(h_\xi)^{-1}(\partial\Phi_2/\partial\xi) + (h_\eta h_\varphi)^{-1}[(\partial/\partial\eta)(h_\varphi A_\varphi)] \text{ by } \xi = \xi_1; \quad (7)$$

$$\Lambda_0 k^2 (\Phi_0 + \Phi_1) = \Lambda_1 k_l^2 \Phi_2 + 2\mu_1 \{ -(h_\xi h_\eta)^{-1}(\partial h_\xi/\partial\eta)[(h_\eta)^{-1}(\partial\Phi_2/\partial\eta) + (h_\xi h_\varphi)^{-1}\partial(h_\varphi A_\varphi)/\partial\xi] + \\ + (h_\xi)^{-1}(\partial/\partial\xi)[-(h_\xi)^{-1}(\partial\Phi_2/\partial\xi) + (h_\eta h_\varphi)^{-1}\partial(h_\varphi A_\varphi)/\partial\eta] \} \text{ by } \xi = \xi_0; \quad (8)$$

$$\Lambda_2 k_l^2 \Phi_3 = \Lambda_1 k_l^2 \Phi_2 + 2\mu_1 \{ -(h_\xi h_\eta)^{-1}(\partial h_\xi/\partial\eta)[(h_\eta)^{-1}(\partial\Phi_2/\partial\eta) + (h_\xi h_\varphi)^{-1}\partial(h_\varphi A_\varphi)/\partial\xi] + \\ + (h_\xi)^{-1}(\partial/\partial\xi)[-(h_\xi)^{-1}(\partial\Phi_2/\partial\xi) + (h_\eta h_\varphi)^{-1}\partial(h_\varphi A_\varphi)/\partial\eta] \} \text{ by } \xi = \xi_1; \quad (9)$$

$$-[(h_\xi h_\eta)^{-1}(\partial h_\eta/\partial\xi) - (h_\xi)^{-1}(\partial/\partial\xi)][(h_\eta)^{-1}(\partial\Phi_2/\partial\eta) + (h_\xi h_\varphi)^{-1}\partial(h_\varphi A_\varphi)/\partial\xi] + [(h_\xi h_\eta)^{-1}(\partial h_\xi/\partial\eta) - \\ - (h_\eta)^{-1}(\partial/\partial\eta)][-(h_\xi)^{-1}(\partial\Phi_2/\partial\xi) + (h_\varphi h_\eta)^{-1}\partial(h_\varphi A_\varphi)/\partial\eta] = 0 \text{ by } \xi = \xi_0 \text{ and } \xi = \xi_1, \quad (10)$$

where $h_\xi = h_0(\xi^2 - \eta^2)^{1/2}(\xi^2 - 1)^{-1/2}$; $h_\eta = h_0(\xi^2 - \eta^2)^{1/2}(1 - \eta^2)^{-1/2}$; $h_\varphi = h_0[(1 - \eta^2)(\xi^2 - 1)]^{1/2}$;

the liquid, Λ_2 is the bulk compression coefficient of the gas filling the shell.

The substitution of series (1) – (5) in boundary conditions (6) – (10) yields an infinite system of equations for determining the desired coefficients. The infinite system is solved by the truncation method. The number of retained terms of expansions (1) – (5) is the greater, the greater the wave size for the given potential.

On the figure 1 are presented the meetings of the modulus $\psi(\theta)$ of the steel gas – filled prolate spheroidal shell with the external coordinate $\xi_1 = 1,005$ and the internal coordinate $\xi_1 = 1,005075$ by the wave dimensions $C : C = 6,75$ (the curve 1), $C = 8,1$ (the curve 2), (curve 3).

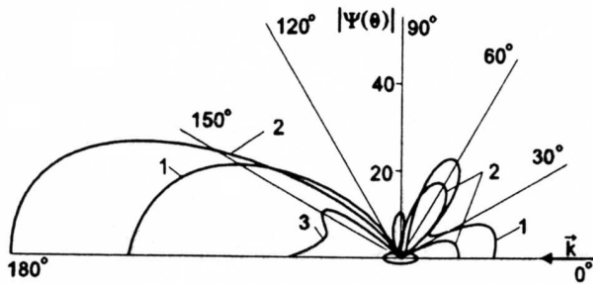


Figure 1. The modulus of the angular characteristics of the scattering $|\psi(\theta)|$ of the elastic (steel) gas-filled spheroidal shell

The scattering of the such form is irradiated by the plane harmonic sound wave of single amplitude. From the figure 1 we see, what the maximum area engages the modulus of the angular characteristics $|\psi(\theta)|$, corresponding to the wave

dimension $C = 2\pi h_0/\lambda = 8,1$ (h_0 is the semi – focal distance of the prolate spheroidal coordinate system, λ is the length of the sound wave in liquid). The meaning $C = 8,1$ is very near to the value $C = 8,25$, corresponding to the resonance of the zero symmetrical Lamb wave[2, 3]. As well we see, the shade lobe of the scattering determined by the angles θ near to 180° grows not monotonously as it is observed by the ideal scatterings, but one may be changed in the any way. For example, by $C = 10,0$ (Figure 1) the shade lobe at the value less, than by $C = 6,75$ and $C = 8,1$. The modulus of the angular characteristics of the sound radiation $|F(\theta)|$ this shell, exciting by the harmonic source, are presented on figure 2 for the wave dimensions $C = 5,7$ (curve 1), $C = 8,1$ (the curve 2), $C = 10,0$ (the curve 3).

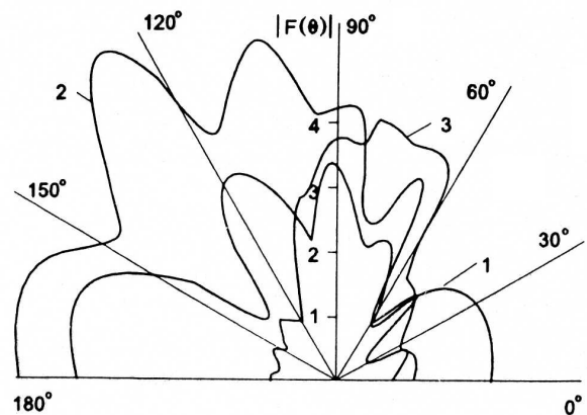


Figure 2. The modulus of the angular characteristics of the radiation $|F(\theta)|$ by the elastic (steel) gas-filled spheroidal shell

And here the picture is repeated: the area under the curve 2 ($C = 8, 1$) is found maximum. So we conclude, that the low frequency resonances of the elastic oscillations may be determined with the help of integral and angular characteristics of the radiation and scattering of the sound by these bodies.

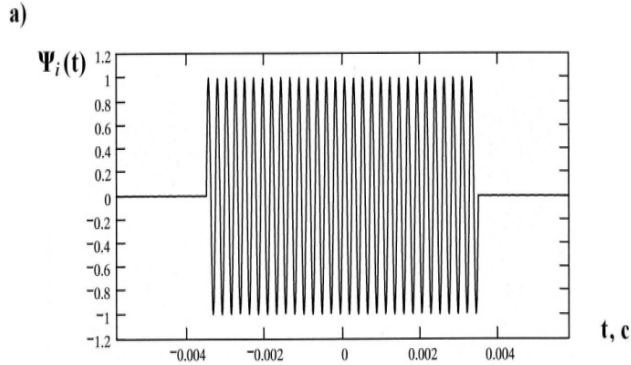
3. The Second of the Article Investigates the Results of Numerical Experiment for Determination of the Low Frequency Resonances of the Elastic Prolate Spheroidal Shell, Irradiating and Establishing by the Pulse Signal

The fallen pulse $\Psi_i(t)$ with the basis frequency $\omega_0 = 2\pi\nu_0$ (Figure 3, a) has the following spectrum $S_0(2\pi\nu)$ (Figure 3, b)[4]:

$$S_0(2\pi\nu) = \int_{\frac{-nT}{2}}^{\frac{+nT}{2}} e^{-i2\pi\nu t} \sin(2\pi\nu_0 t) dt \quad (11)$$

$$= \frac{i\nu_0}{\pi(\nu_0^2 - \nu^2)} (-1)^n \sin(\pi n \nu / \nu_0),$$

where: T – the period of the harmonic signal with the frequency ν_0 , $T = 1/\nu_0$; n – number of the periods in



pulse; ν – the current circular frequency.

The spectrum $S_0(2\pi\nu)$ connects with by the return Fourier transform[4]:

$$\Psi_i(t) = \frac{1}{\pi} \operatorname{Re} \int_0^\infty S_0(2\pi\nu) e^{+i2\pi\nu t} d(2\pi\nu). \quad (12)$$

With the help $S_s(2\pi\nu)$ and $S_\Sigma(2\pi\nu)$ found the pulses $\Psi_s(t)$ and $\Psi_\Sigma(t)$ (scattered and diffracted according)[4 – 15]:

$$\Psi_s(t) = \frac{1}{\pi} \operatorname{Re} \int_0^\infty S_s(2\pi\nu) e^{+i2\pi\nu t} d(2\pi\nu). \quad (13)$$

$$\Psi_\Sigma(t) = \frac{1}{\pi} \operatorname{Re} \int_0^\infty S_\Sigma(2\pi\nu) e^{+i2\pi\nu t} d(2\pi\nu). \quad (14)$$

For the computation of the spectrums $S_s(2\pi\nu)$ and $S_\Sigma(2\pi\nu)$ are used the amplitude – phase characteristics of the sound scattering at spheroidal shell by the stationary (harmonic) irradiation[2].

At the Figure 4, 5 and 6 were representing the pulses of the back scattering $\Psi_s(t)$ (a) and the normalized modulus of the spectrums $|S_s(\nu)|$ of the pulses $\Psi_s(t)$ on the resonances (Figure 5 and 6) and outside of the resonance (Figure 4).

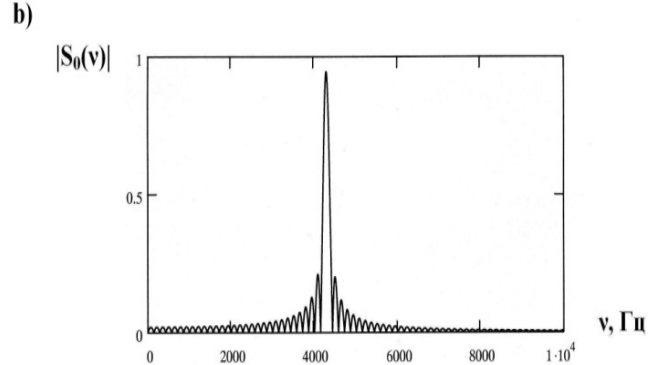


Figure 3. The fallen pulse $\Psi_i(t)$ (a); the modulus of the spectrum $|S_0(\nu)|$ of the pulse $\Psi_i(t)$ (b)

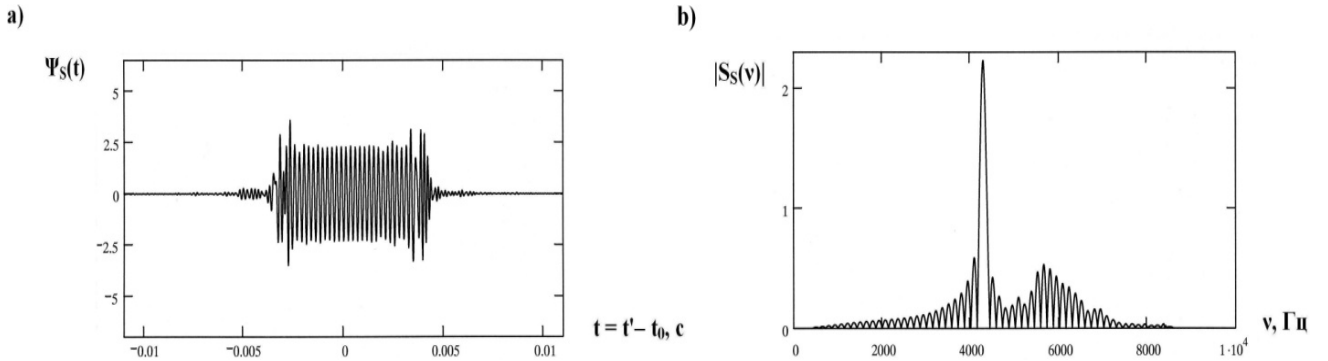


Figure 4. The pulse of the back scattering $\Psi_s(t)$ (a); the normalized modulus of the spectrum $|S_s(\nu)|$ of the pulse $\Psi_s(t)$ (b); $c = 5, 0$; $\theta_0 = 0^\circ$; $\theta = 0^\circ$

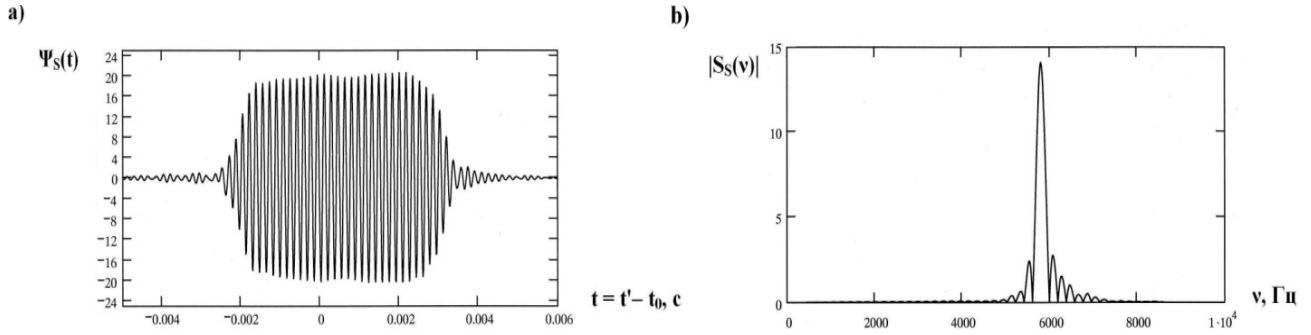


Figure 5. The pulse of the back scattering $\Psi_s(t)$ (a); the normalized modulus of the spectrum $|S_s(\nu)|$ of the pulse $\Psi_s(t)$ (b); $c = 6,75$; $\theta_0 = 0^\circ$; $\theta = 0^\circ$

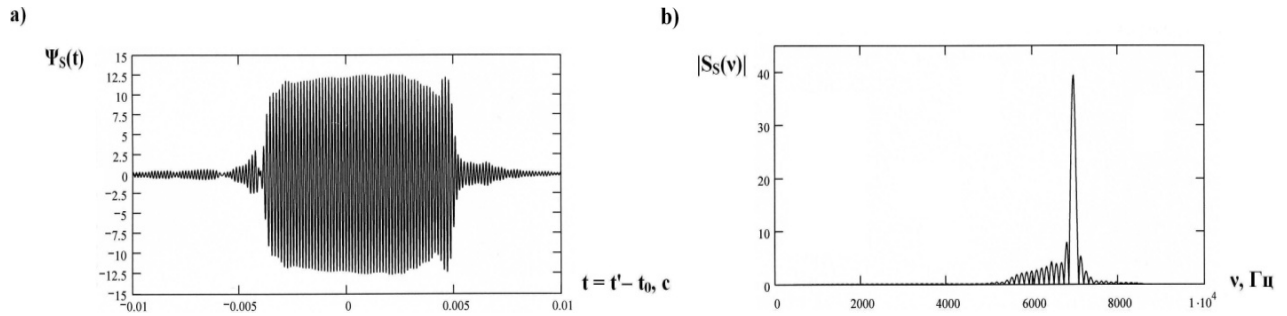


Figure 6. The pulse of the back scattering $\Psi_s(t)$ (a); the normalized modulus of the spectrum $|S_s(\nu)|$ of the pulse $\Psi_s(t)$ (b); $c = 8,1$; $\theta_0 = 0^\circ$; $\theta = 0^\circ$

At Figure 7, 8 and 9 were representing the scattered pulses $\Psi_s(t)$ in the direction $\theta = 180^\circ$ and them the normalized modulus on the resonances (Figure 8 and 9) and outside resonance (Figure 7).

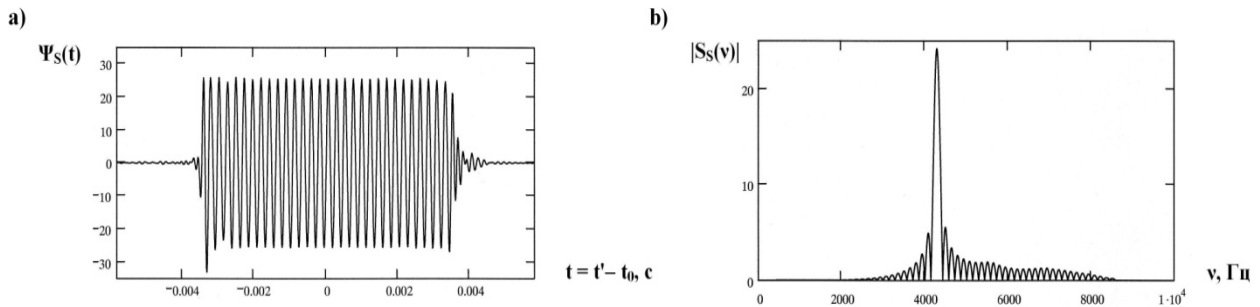


Figure 7. The scattered pulse $\Psi_s(t)$ in the direction $\theta = 180^\circ$ (a); the normalized modulus of the spectrum $|S_s(\nu)|$ of the pulse $\Psi_s(t)$ (b); $c = 5,0$; $\theta_0 = 0^\circ$

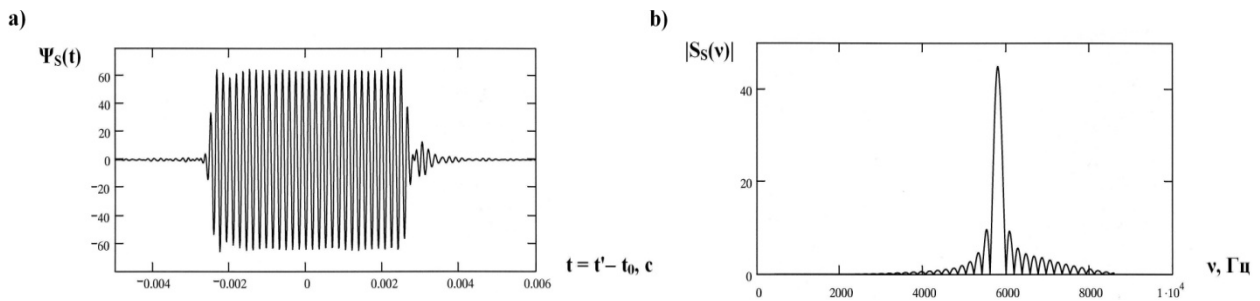


Figure 8. The scattered pulse $\Psi_s(t)$ in the direction $\theta = 180^\circ$ (a); the normalized modulus of the spectrum $|S_s(\nu)|$ of the pulse $\Psi_s(t)$ (b); $c = 6,75$; $\theta_0 = 0^\circ$

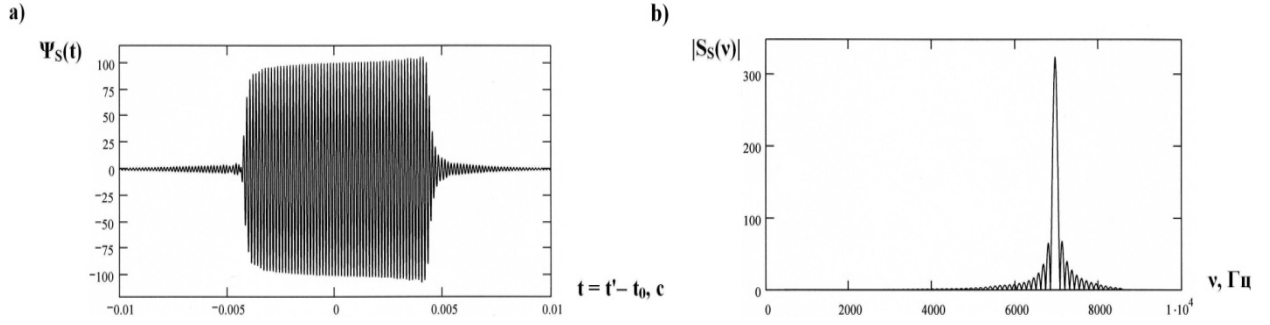


Figure 9. The scattered pulse $\Psi_s(t)$ in the direction $\theta = 180^\circ$ (a); the normalized modulus of the spectrum $|S_s(\nu)|$ of the pulse $\Psi_s(t)$ (b); $c = 8, 1$; $\theta_0 = 0^\circ$

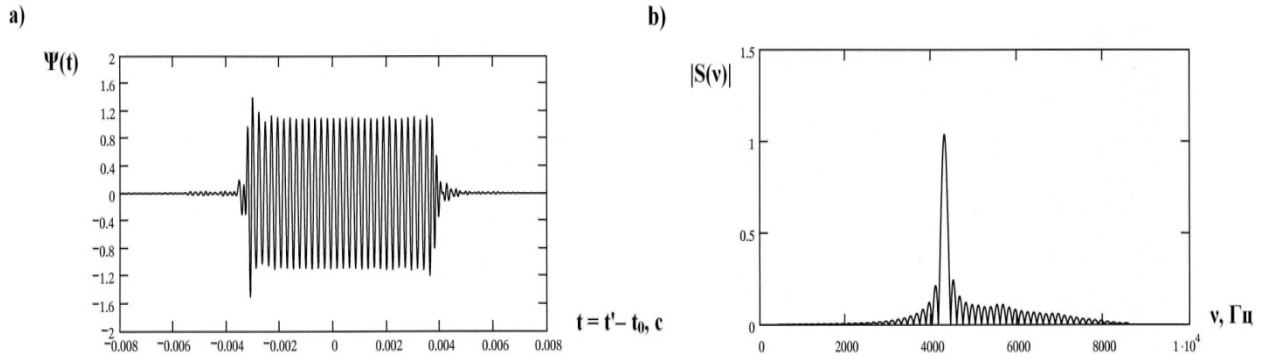


Figure 10. The radiated pulse $\Psi(t)$ in the direction $\theta = 180^\circ$ (a); the normalized modulus of the spectrum $|S(\nu)|$ of the pulse $\Psi(t)$ (b); $c = 5, 0$; $\theta_0 = 0^\circ$

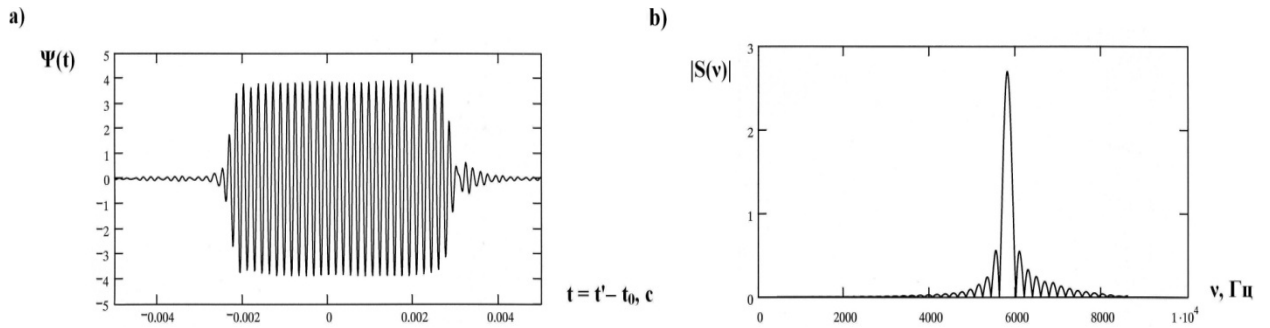


Figure 11. The radiated pulse $\Psi(t)$ in the direction $\theta = 180^\circ$ (a); the normalized modulus of the spectrum $|S(\nu)|$ of the radiated pulse $\Psi(t)$ (b); $c = 6, 75$; $\theta_0 = 0^\circ$

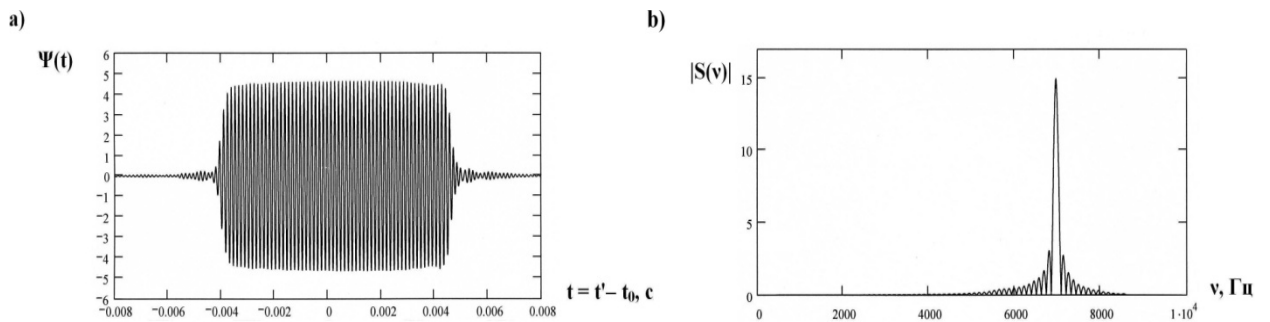


Figure 12. The radiated pulse $\Psi(t)$ in the direction $\theta = 180^\circ$ (a); the normalized modulus of the spectrum $|S(\nu)|$ of the radiated pulse $\Psi(t)$ (b); $c = 8, 1$; $\theta_0 = 0^\circ$

At Figure 10, 11 and 12 were representing the radiated pulses $\Psi(t)$ in the direction $\theta = 180^\circ$ and them the normalized moduluses on the resonances (Figure 11 and 12) and outside resonance 9 Figure 10).

From the comparison of these figures we see, what the amplitudes of the pulses on the resonances much higher.

4. Conclusions

With help of the numerical experiment are found the low frequency resonances of the elastic spheroidal shell by the axis – symmetrical illumination.

ACKNOWLEDGMENTS

This work was supported as part of research under State Contract no P242 of April 21. 2010, within the Federal Target Program “Human Capital in Science and Education for Education for Innovative Russia, 2009 – 2013”.

REFERENCES

- [1] A.A. Kleshchev. J. Techn. Acoust. 2, 27 (1995).
- [2] A.A. Kleshchev. Hydroacoustic Scatterers (Prima, St. Petersburg, 2012)[in Russia].
- [3] A.A. Kleshchev. Phys. Acoust. 38, 361 (1992).
- [4] A.A. Kharceovich. Spectrum and Analysis. (GITTL, Moskau, 1957)[in Russia].
- [5] Gaunard G. C., Werby M. F. J. A. S. A. 77, 2081 (1985).
- [6] Werby M. F., Gaunard G. C. J. A. S. A. 82, 1369 (1987).
- [7] Werby M. F., Green L. H. J. A. S. A. 74, 625 (1983).
- [8] Werby M. F., Green L. H. J. A. S. A. 76, 1227 (1984).
- [9] Werby M. F., Green L. H. J. A. S. A. 81, (1987).
- [10] Werby M. F., Tango G. J. J. A. S. A. 79, 1260 (1986).
- [11] A. A. Kleshchev. Sov. Phys. Acoust. 57, 381 (2011).
- [12] A. A. Kleshchev, E. I. Kuznetsova. Phys. Acoust. 57,495 (2011).
- [13] A. A. Kleshchev. Diffraction and Propagation of Waves in Elastic Mediums and Bodies. (Vlas, St.- Petersburg, 2002)[in Russian].
- [14] A. A. Kleshchev. Diffraction, Radiation and Propagation of Elastic Waves. (Profpriint, St.- Petersburg, 2006)[in Russian].
- [15] A. A. Kleshchev. Phys. Acoust. 58, 338 (2012).